Inorg. Chem. **2004**, *43*, 5393–5402

Mechanisms of Ferriheme Reduction by Nitric Oxide: Nitrite and General Base Catalysis[1]

Bernadette O. Fernandez, Ivan M. Lorkovic, and Peter C. Ford*

Department of Chemistry and Biochemistry, University of California, Santa Barbara, Santa Barbara, California 93106-9510

Received April 9, 2004

The reductive nitrosylation ($Fe^{III}(P) + 2NO + H_2O = Fe^{II}(P)(NO) + NO_2^- + 2H^+$) of the ferriheme model Fe^{III}(TPPS) (TPPS = tetra(4-sulfonatophenyl)porphyrinato) has been investigated in moderately acidic solution. In the absence of added or adventitious nitrite, this reaction displays general base catalysis with several buffers in aqueous solutions. It was also found that the nitrite ion, NO_2^-, is a catalyst for this reaction. Similar nitrite catalysis was demonstrated for another ferriheme model system Fe^{III}(TMPy) (TMPy = *meso*-tetrakis(*N*-methyl-4-pyridyl)porphyrinato), and for ferriheme proteins met-hemoglobin (metHb) and met-myoglobin (metMb) in aqueous buffer solutions. Thus, it appears that such catalysis is a general mechanistic route to the reductive nitrosylation products. Two nitrite catalysis mechanisms are proposed. In the first, NO_2^- is visualized as operating via nucleophilic addition to the Fe^{III}-coordinated NO in a manner similar to the reactions proposed for Fe^{III} reduction promoted by other nucleophiles. This would give a labile N_2O_3 ligand that hydrolyzes to nitrous acid, regenerating the original nitrite. The other proposal is that Fe^{III} reduction is effected by direct outer-sphere electron transfer from NO_2^- to $Fe^{III}(P)(NO)$ to give nitrogen dioxide plus the ferrous nitrosyl complex $Fe^{II}(P)(NO)$. The NO_2 thus generated would be trapped by excess NO to give N_2O_3 and, subsequently, nitrite. It is found that the nitrite catalysis rates are markedly sensitive to the respective $Fe^{III}(P)(NO)$ reduction potentials, which is consistent with the behavior expected for an outer-sphere electron-transfer mechanism. Nitrite is the product of NO autoxidation in aqueous solution and is a ubiquitous impurity in experiments where aqueous NO is added to an aerobic system to study biological effects. The present results demonstrate that such an impurity should not be assumed to be innocuous, especially in the context of recent reports that endogenous nitrite may play physiological roles relevant to the interactions of NO and ferriheme proteins.

Introduction

Nitric oxide (nitrogen monoxide) is known to play key roles in a variety of mammalian physiological processes,[2,3] including blood pressure control, neurotransmission, and immune response, and numerous disease states involving NO imbalances have been identified.[3,4] Much of the mammalian biology of NO can be attributed to reactions with metal centers such as hemes; thus, it is important to understand the fundamental mechanisms of such processes. One such reaction is reductive nitrosylation, a process whereby the NO reduction of the metal is concomitant with the nitrosation of a nucleophile (eq 1). This has been demonstrated in several ferriheme proteins including met-hemoglobin (metHb),[5,6]

* Author to whom correspondence should be addressed. E-mail: ford@chem.ucsb.edu.

(1) Aspects of the work reported here have appeared in preliminary communications. (a) Fernandez, B. O.; Lorkovic, I. M.; Ford, P. C. *Inorg. Chem.* **2003**, *42*, 2−4. (b) Fernandez, B. O.; Ford, P. C. *J. Am. Chem. Soc.* **2003**, *125*, 10510−10511.

(2) (a) Moncada, S.; Palmer, R. M. J.; Higgs, E. A. *Pharmacol. Rev.* **1991**, *43*, 109−142. (b) Feldman, P. L.; Griffith, O. W.; Stuehr, D. J. *Chem. Eng. News* **1993**, *71*, 26. (c) Butler, A. R.; Williams, D. L. *Chem. Soc. Rev.* **1993**, 233−241. (d) Feelisch, M., Stamler, J. S., Eds. *Methods in Nitric Oxide Research*; John Wiley and Sons: Chichester, England, 1996, and references therein. (e) Wink, D. A.; Hanbauer, I.; Grisham, M. B.; Laval, F.; Nims, R. W.; Laval, J.; Cook, J.; Pacelli, R.; Liebmann, J.; Krishna, M.; Ford, P. C.; Mitchell, J. B. *Curr. Top. Cell. Regul.* **1996**, *34*, 159−187.

(3) Ignarro, L. J., Ed. *Nitric Oxide: Biology and Pathobiology*; Academic Press: San Diego, CA, 2000.

(4) Fang, F. C., Ed. *Nitric Oxide and Infection*; Kluwer Academic/Plenum Publishers: New York, 1999.

(5) (a) Chien, J. C. W. *J. Am. Chem. Soc.* **1969**, *91*, 2166−2168. (b) Ford, P. C.; Lorkovic, I. M. *Chem. Rev.* **2002**, *102*, 993−1017. (c) Reichenbach, G.; Sabatini, S.; Palombari, R.; Palmerini, C. A. *Nitric Oxide* **2001**, *5*, 395−401. (d) Cabail, M. Z.; Pacheco, A. A. *Inorg. Chem.* **2003**, *42*, 270−272. (e) Ford, P. C.; Laverman, L. E.; Lorkovic, I. M. *Adv. Inorg. Chem.* **2003**, *54*, 203−257.

(6) Hoshino, M.; Maeda, M.; Konishi, R.; Seki, H.; Ford, P. C. *J. Am. Chem. Soc.* **1996**, *118*, 5702−5707.

10.1021/ic049532x CCC: $27.50 © 2004 American Chemical Society
Published on Web 07/29/2004

Scheme 1. Proposed Ferrihemeprotein Reductive Nitrosylation at pH > 7 [6]

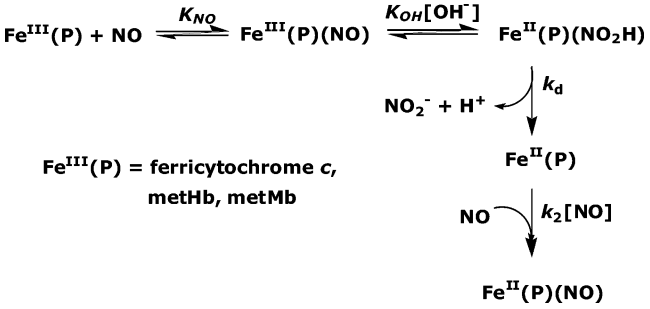

cupric centers in cytochrome *c* oxidase and laccase, and Cu(II) and Fe(III) model systems.[7,8] Reductive nitrosylation has also received attention as a possible pathway for the formation of biological *S*-nitrosothiols and *N*-nitrosoamines.[9] In addition, it has been suggested that such a pathway may be responsible for the nitrosation of the β-cys-93 of hemoglobin to form *S*-nitrosohemoglobin (SNO-Hb),[10] the subject of a controversial proposal as a nitric oxide carrier in the cardiovascular system.[11]

$$L_xM^{n+} + NO + Nuc \rightleftharpoons L_xM^{(n-1)} + Nuc{-}NO^+ \quad (1)$$

In an earlier investigation, Hoshino and co-workers[6] reported the kinetics for the NO reductions of ferriheme proteins, ferric cytochrome-*c* (Cyt^{III}), met-myoglobin (metMb), and met-hemoglobin in buffered aqueous media. At pH values >6.5, the rates of these reactions displayed a first-order dependence on [OH^-] and a complex dependence on [NO], consistent with the equilibrium formation of the nitrosyl complex $Fe^{III}(NO)$ followed by the nucleophilic attack of OH^- at the coordinated nitrosyl (Scheme 1). Such coordination leads to charge transfer from the NO to the Fe(III) center,[12] rendering the nitrosyl more electrophilic than the free ligand.

The rate law predicted by Scheme 1 is described by eq 2, and the observed rates for the NO reduction of Cyt^{III}, metMb, and metHb proved to be functions of both [NO] and [OH^-] in accord with this analysis.

$$\frac{d[Fe^{III}]}{dt} = -k_d \times \frac{K_{NO}[NO]}{1 + K_{NO}[NO]} \times \frac{K_{OH}[OH^-]}{1 + K_{OH}[OH^-]}[Fe^{III}] \quad (2)$$

However, metHb also demonstrated a pH-independent pathway for reductive nitrosylation at lower pH values (<6) ($k_{H_2O} = 1.1 \times 10^{-3}$ s^{-1}),[6] possibly the result of the metHb(NO) reaction with water that is activated by general base catalysis. It was in this context that the research described here was initiated to determine whether analogous general base catalysis pathways are apparent in the NO reductions of water-soluble ferriheme models such as $Fe^{III}(TPPS)(H_2O)_2$ (**1**, TPPS = tetra(4-sulfonato-phenyl)-porphyrinato) in aqueous buffered solutions (eq 3). General base catalysis is indeed demonstrated; however, perhaps an even more interesting discovery is that the nitrite ion (NO_2^-) strongly catalyzes this reaction. This catalytic pathway also extends to another ferriheme model, $Fe^{III}(TMPy)(H_2O)_2$ (**2**, TMPy = *meso*-tetrakis(*N*-methyl-4-pyridyl)porphyrinato), and to the ferriheme proteins metMb and metHb.

$$Fe^{III}(TPPS) + 2\,NO + H_2O \rightleftharpoons Fe^{II}(TPPS)(NO) + NO_2^- + 2H^+ \quad (3)$$

As noted above, the transfer of NO^+ from the heme iron to a β-cys-93 in the hemoglobin analogous to the reaction shown in eq 1 was proposed as a possible mechanism for the formation of SNO-Hb.[10] This proposal is similar to the report that the oxidized myoglobin (metMb) reacts with NO plus glutathione (GSH) to give *S*-nitrosoglutathione (GSNO).[5c] However, it has also been argued that the formation of SNO-Hb may be the result of mixing artifacts when NO is added to ferriheme protein or red blood cell solutions, especially when dioxygen is present.[13] A related issue is the recent attention directed toward the possible role of the nitrite ion (NO_2^-) in the cardiovascular system.[14] Because nitrite is reported to be a major vascular storage pool of NO_x species,[14] the chemical interplay of ferriheme models and proteins with NO and nitrite continues to be an issue of major importance to cardiovascular biology.

Experimental Section

Materials. All solutions were prepared with doubly distilled water from a Nanopure distillation system. The iron(III) porphyrin salts ($Na_4[Fe^{III}(TPPS)]$ and $[Fe^{III}(TMPy)(Cl)]Cl_4$) were obtained from Midcentury (Posen, IL), human hemoglobin (Hb) was obtained from Sigma, and horse skeletal myoglobin (Mb) was obtained from Calbiochem. Reagent-grade sodium nitrite (Fisher Scientific) was used without further purification. Buffer solutions were prepared from sodium bisulfate ($NaHSO_4 \cdot H_2O$ (Allied Chemical) (pH 2

(7) (a) Torres, J.; Cooper, C. E.; Wilson, M. T. *J. Biol. Chem.* **1998**, *273*, 8756−8766. Torres, J.; Svistunenko, D.; Karlsson, B.; Cooper, C. E.; Wilson, M. T. *J. Am. Chem. Soc.* **2002**, *124*, 963−967. (c) Tran, D.; Skelton, B. W.; White, A. H.; Laverman, L. E.; Ford, P. C. *Inorg. Chem.* **1998**, *37*, 2505−2511.

(8) For example, (a)Wayland, B. B.; Olson, L. W. *J. Am. Chem. Soc.* **1974**, *96*, 6037−6041. (b) Trofimova, N. S.; Safronov, A. Y.; Ikeda, O. *Inorg. Chem.* **2003**, *42*, 1945−1951.

(9) (a) Feelisch, M. S.; Rassaf, T.; Mnaimneh, S.; Singh, N.; Byran, N. S.; Jourd'Heuil, D.; Kelm, M. *FASEB J.* **2002**, *16*, 1775−1785 (b) Bryan, N. S.; Rassaf, T.; Maloney, R. E.; Rodriguez, C. M.; Saijo, F.; Rodriguez, J. R.; Feelisch, M. *Proc. Nat. Acad. Sci. U.S.A.* **2004**, *101*, 4308−4313.

(10) Luchsinger, B. P.; Rich, E. N.; Gow, A. J.; Williams, E. M.; Stamler, J. S.; Singel, D. J. *Proc. Natl. Acad. Sci. U.S.A.* **2003**, *100*, 461−466.

(11) (a) Jia, L.; Bonaventura, C.; Bonaventura, J.; Stamler, J. S. *Nature* **1996**, *380*, 221−226. (b) Gow, A. J.; Luchsinger, B. P.; Pawloski, J. R.; Singel, D. J.; Stamler, J. S. *Proc. Natl. Acad. Sci. U.S.A.* **1999**, *96*, 9027−9032. (c) See also Gladwin, M. T.; Lancaster, J. R., Jr.; Freeman, B. A.; Schechter, A. N. *Nat. Med. (N.Y.)* **2003**, *9*, 496−500.

(12) (a) Scheidt, W. R.; Lee, Y. J.; Hatano, K. *J. Am. Chem. Soc.* **1984**, *106*, 3191−3198. (b) Wylie, G. R. A.; Scheidt, W. R. *Chem. Rev.* **2002**, *102*, 106−1089.

(13) (a) Han, T. H.; Hyduke, D. R.; Vaughn, M. W.; Fukuto, J. M.; Liao, J. C. *Proc. Natl. Acad. Sci. U.S.A.* **2002**, *99*, 7763−7768. (b) Zhang, Y.; Hogg, N. *Free Radical Biol. Med.* **2002**, *32*, 1212−1219. (c) Herold, S.; Rock, G. *J. Biol. Chem.* **2003**, *278*, 6623−6634.

(14) (a) Cosby, K.; Partovi, K. S.; Patel, R. P.; Reiter, C. D.; Martyr, S.; Yang, B. K.; Waclawiw, M. A.; Zaloa, G.; Xu, X.; Huang, K. T.; Shields, H.; Kim-Shapiro, D. B.; Schechter, A. N.; Cannon, R. O., III; Gladwin, M. T. *Nat. Med. (N.Y.)* **2003**, *9*, 1498−1505. We thank Dr. M. T. Gladwin for an advance copy of this manuscript. (b) Rodriquez, J.; Maloney, R. E.; Rassaf, T.; Bryan, N. S.; Feelisch, M. *Proc. Natl. Acad. Sci. U.S.A.* **2003**, *100*, 336−341.

solutions)), chloroacetic acid (Mallinckrodt) (pH 3), sodium acetate, (Mallinckrodt) mixed with triflic acid (CF_3SO_3H) (Aldrich) (pH 4−5), *N*,*N*′-diethyl-*N*,*N*′-bis(sulfopropyl)ethylenediamine, DESPEN ($HO_3SC_3H_6$)(C_2H_5)$NC_2H_4N(C_2H_5)$−(C_3H_6−SO_3H) (GFS Chemicals) (pH 4.5−6), and NaH_2PO_4/Na_2HPO_4 (Fisher Scientific) (pH 6−7.4).

Chromatographic-grade argon (Praxair) was passed through an Oxiclear oxygen trap (Alltech) before use to provide an inert atmosphere. Nitric oxide (99%, Aire Liquide) was purified by passage through a stainless steel column filled with Ascarite II (Thomas Scientific) to remove higher nitrogen oxides. All NO transfers were carried out on a greaseless vacuum line.

General Methods. The purchased hemoglobin and myoglobin samples were mixtures of oxidized hemo/myoglobin and the oxy form of reduced hemo/myoglobin.[15] To obtain purified metHb, we subjected the solutions to gentle degassing on a vacuum line because removing dioxygen from the solutions stabilizes the oxidized form of the protein.[15b] Another method to obtain metHb is to react the protein solution with excess of $K_3[Fe(CN)_6]$ (Mallinckrodt) to oxidize the remaining Hb in the sample.[15c] The metHb solution was then purified via molecular exclusion chromatography by passing through a column of CM Sephadex C-25 resin (Pharmacia). Purified metMb was obtained by analogous procedures.

Buffer solutions were prepared according to standard procedures. Unless otherwise noted, solutions were also adjusted to a common ionic strength (μ), generally 0.10 M, by adding sodium triflate, $Na[CF_3SO_3]$ (Aldrich), as the supporting electrolyte. Dilute solutions of triflic acid were added to the reaction solutions to adjust the pH.

Aqueous solutions for kinetics measurements were deaerated. Iron porphyrin solutions were subject to at least three freeze−pump−thaw cycles (f−p−t) using specialized cells described below. Because ferriheme proteins denature under the temperature extremes of the f−p−t cycles, we degassed them via boiling under reduced pressure (evacuating the samples on the vacuum manifold for several cycles at room temperature).

NO solutions for kinetics studies were prepared by vacuum transfer techniques using flasks of known volumes with greaseless fittings, high-vacuum Teflon stopcocks, a four-sided quartz cuvette, a septum-sealed electrode adaptor (as injection ports) for anaerobic use, and an O-ring adaptor for the connection to the gas/vacuum manifold. All manipulations of NO gas and NO-containing solutions were carried out on vacuum lines using stainless steel or glass with greaseless fittings. When necessary, NO samples were passed through a secondary flask containing additional Ascarite II or 6 M NaOH to remove other NO_x species. The NO was frozen at 77 K into this secondary scrubber, and then the cleaned NO was quantitatively distilled into the desired reaction flask after the secondary flask was thawed. After NO transfer, the flask contents were thawed and shaken for equilibration. NO concentrations were calculated from P_{NO} and the assumption that the solubility is the same as it is in water.[16]

Solutions for stopped-flow experiments were transferred from the equilibrated reaction flasks and loaded onto the evacuated drive syringes via argon-purged airtight syringes (Hamilton Gastight no. 1010 or no. 1005) equipped with removable needles, Teflon plungers, and exit valves. All solutions were protected from room light with aluminum foil or a black cloth and were used within the same day of preparation.

Instrumentation. The solution pH was monitored using a deep-vessel, Corning combination electrode with a silver ion barrier (model 476306). The pH meter (Orion Research) and electrode were calibrated over the pH 4−10 range with standard buffers (EM Science and Fisher Scientific). Electronic absorption spectra and kinetics measurements (Agilent Chemstation) were recorded on a Hewlett-Packard 8452A diode array spectrophotometer using custom-made reaction vessels equipped with 1.0-cm quartz cells (NSG Precision Cells and Hellma). All kinetics analyses and measurements were made using a thermostated cell holder attached to a cell stirring module that was controlled by a temperature bath to ensure proper equilibration and mixing of solutions while data was being accumulated. Other kinetics measurements were performed with an Applied Photophysics model SX-18 MV stopped-flow spectrometer using standard mixing techniques. Drive syringes were thoroughly purged with the appropriate solutions after degassing, and samples were equilibrated for 15−30 min at the appropriate temperature using the attached temperature control unit.

Data Analysis. Absorbance intensity versus time traces obtained by single-wavelength detection from all instruments were converted to ΔAbs versus time plots and were fit to appropriate kinetics models using Igor 4.0 (Wavemetrics) software.

Results and Discussion

Proton-Coupled Redox Potentials. The redox reaction depicted in eq 3 can be separated into the equilibrium formation of the ferriheme nitrosyl complexes (eq 4) and the subsequent redox reaction (eq 5). The potential for the latter is drawn from the half cells shown in eqs 6 and 7.[17] A key feature is the marked acid dependence of the NO_2^-/NO half cell ($E° = 1.20$ V).[18] Under standard conditions (1 N H^+), the NO reductions of neither Fe^{III}(TPPS)(NO) nor Fe^{III}(TMPy)(NO) are favorable ($\Delta E° = -0.62$ and -0.42 V, respectively, for eq 5); however, in both cases, the reaction becomes favorable at higher pH values ($\Delta E = 0.21$ and 0.41 V, respectively, at pH 7) and at lower nitrite concentrations. In this context, kinetics experiments with these two ferriheme model systems were carried out at pH > 3 but at pH < 6 to suppress the hydrolysis of Fe^{III}-coordinated H_2O and the formation of oxo-bridged dimers $Fe^{III}OFe^{III}$.[17,19,20]

$$Fe^{III}(P) + NO \overset{K_{NO}}{\rightleftharpoons} Fe^{III}(P)(NO) \quad (4)$$

$$Fe^{III}(P)(NO) + H_2O + NO \rightleftharpoons Fe^{II}(P)(NO) + NO_2^- + 2H^+ \quad (5)$$

$$Fe^{III}(P)(NO) + e^- \rightleftharpoons Fe^{II}(P)(NO) \quad (6)$$

$$NO_2^- + 2H^+ + e^- \rightleftharpoons H_2O + NO \quad (7)$$

In the context of the above discussion, it is notable that Fe^{III}(TPPS) solutions prepared at pH 2.04 (100 mM bisulfate)

(15) (a) Information from the Sigma-Aldrich website (www.sigma-aldrich.com) and from Sigma-Aldrich customer service/technical support. (b) Budavari, S., Ed. *Merck Index: An Encycopedia of Chemicals, Drugs, and Biologicals*, 11th ed.; Merck & Co: Rahway, NJ, 1989; p 734. (c) Joshi, M. S.; Ferguson, T. B., Jr.; Han. T. H.; Hyduke, D. R.; Liao, J. C.; Rassaf, T.; Bryan, N.; Feelisch, M.; Lancaster, J. R., Jr. *Proc. Natl. Acad. Sci. U.S.A.* **2002**, *99*, 10341−10346.

(16) Young, C. L., Ed. *Oxides of Nitrogen*; *IUAPC Solubility Data Series*; Pergamon Press: Oxford, U.K., 1983; Vol. 8.

(17) (a) Barley, M. H.; Takeuchi, K. J.; Meyer, T. J. *J. Am. Chem. Soc.* **1986**, *108*, 5876−5885. (b) Barley, M. H.; Rhodes, M. R.; Meyer, T. J. *Inorg. Chem.* **1987**, *26*, 1746−1750.

(18) Bard, A. J., Parsons, R., Jordan, J., Eds. *Standard Potentials in Aqueous Solutions*; Marcel Dekker: New York, 1985; pp 127−139.

demonstrated no reduction by NO (1.9 mM), whereas a pH 3.06 solution (100 mM monochloroacetic acid) exhibited minimal spectral changes.

The equilibrium constant for eq 3 was determined for Fe^{III}(TPPS) in 298 K, pH 4.5 NaOAc/HOAc buffer (50 mM) with [NO] = 1.9 mM by recording spectral changes as the nitrite concentration was varied from 0 to 40 mM (Supporting Information, Figure S1). From these spectral changes and a Lineweaver−Burke-type analysis, the equilibrium constant was determined to be $(3.35 \pm 0.89) \times 10^{-2}$ M. From this value, the reduction potential for eq 6 (P = TPPS) was found to be (0.582 ± 0.007) V, a value that compares well with that (0.586 V) determined by Meyer and co-workers using cyclic voltammetry.[17a]

Equilibrium Formation of Fe^{III}(P)(NO). Upon mixing a solution of Fe^{III}(TPPS) (**1**) with NO, the equilibrium formation of Fe^{III}(TPPS)(NO) (**3**) is evident in the shift of the Soret band λ_{max} at 394 nm ($\epsilon = 9.7 \times 10^4$ M^{-1} cm^{-1}) characteristic of **1** to the λ_{max} (422 nm, $\epsilon = 12.0 \times 10^4$ M^{-1} cm^{-1}) characteristic of **3**. At low pH (<3), no significant further reaction is observed. At higher pH values, there is a progressive change in the spectrum both in the Soret and Q-band regions consistent with the reduction of **3** to Fe^{II}(TPPS)(NO) (**4**) (λ_{max}(Soret) = 412 nm, $\epsilon = 10.0 \times 10^4$ M^{-1} cm^{-1}) as indicated by eq 5 (Supporting Information, Figure S2). Because the second reaction under these conditions is slow, it is possible to evaluate the equilibrium represented by eq 4 from the spectral changes observed upon changing the NO partial pressure for pH 5 buffered solutions (μ = 0.10 M) at 298 K. The value of $(1.32 \pm 0.09) \times 10^3$ M^{-1} determined for K is in good agreement with the previously reported values of $(1.2 \pm 0.2) \times 10^3$ M^{-1} and 1.1×10^3 M^{-1} in acidic solution.[21]

Because the rate constants for the NO reduction of Fe^{III}(TMPy) (**2**) proved to be much larger than those for Fe^{III}(TPPS) (10^{-3} vs 10^{-4} s^{-1}), the equilibrium constant for NO association was determined at lower pH, where the ferric nitrosyl species would be stable. In pH 1.0 (μ_{tot} = 0.10 M, using 100 mM triflic acid) aqueous solution, the equilibrium constant for eq 4 at 298 K was determined for Fe^{III}(TMPy) from the changes in the absorption spectrum as NO was added. Spectrophotometric determination of K_{NO} in this manner gave $(4.6 \pm 1.7) \times 10^2$ M^{-1} (Figure 1), roughly a factor of 3 smaller than the K_{NO} determined for **1**.

An alternative way to measure K_{NO} is to determine the rate constants, k_{obs}, for the approach to equilibrium concentrations of the Fe^{III}(P)(NO) and Fe^{III}(P) complexes after mixing solutions of Fe^{III}(P) and of NO. The observed rate constant is equal to the sum of k_{on}[NO] + k_{off}, where k_{on} and k_{off} are the respective rate constants for the formation and dissociation of Fe(P)(NO) (eq 8).[22] Stopped-flow kinetics

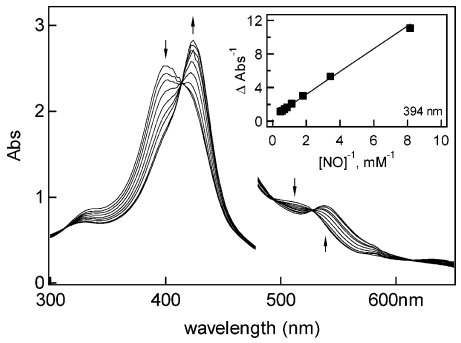

Figure 1. Spectral changes upon adding different [NO] to an aqueous solution of Fe^{III}(TMPy) with 100 mM triflic acid (μ_{tot} = 0.10 M) at 298 K. The inset is a linear plot of ΔAbs^{-1} (at 394 nm) versus $[NO]^{-1}$ from which the equilibrium constant $K_{NO} = (4.6 \pm 1.7) \times 10^2$ M^{-1} was calculated.

techniques were used to measure the k_{obs} for the reaction of NO with Fe^{III}(TMPy) for four different [NO] ((0.20−1.0 mM) at pH 1.0, μ = 0.10) and T = 298 K. The k_{obs} values determined by monitoring the temporal spectral changes at 542 nm were plotted versus [NO] to give linear plots (data not shown) with slopes equal to k_{on} (2.9×10^4 M^{-1} s^{-1}) and intercepts equal to k_{off} (68 s^{-1}). Interestingly, both k_{on} and k_{off} in this case are significantly smaller than the analogous rate constants measured for **1** (5×10^5 M^{-1} s^{-1} and 460 s^{-1}, respectively) by laser flash photolysis techniques under comparable conditions.[21a] The equilibrium constant K_{NO} obtained from the ratio of these values was 4.2×10^2 M^{-1}, in agreement with that determined spectroscopically.

$$Fe^{III}(P) + NO \underset{k_{off}}{\overset{k_{on}}{\rightleftharpoons}} Fe^{III}(P)(NO) \qquad (8)$$

The values of K_{NO} for ferriheme proteins metHb and metMb have been previously reported as 1.4×10^4 and 1.3×10^4 M^{-1}, respectively, in buffered solutions at pH 7.[21,23]

NO Reduction of Fe^{III}(TPPS). General Base Catalysis. The kinetics for the NO reduction and nitrosylation of **1** to **4** were investigated over pH range 3−6 using various buffers at 298 K. Under these conditions, μ-oxo dimerization of Fe^{III}(TPPS) is minimal. Equilibrating a buffered aqueous solution of **1** with NO (760 Torr, [NO] = 1.9 mM) led to the rapid formation of an equilibrium mixture of **1** and the ferric nitrosyl complex **3** (eq 4), followed by the slower reduction to the ferrous analogue **4** (eq 5). The solution spectra exhibited a corresponding shift in the Soret band λ_{max} from 422 to 412 nm. The Q-band region also exhibited temporal changes that are characteristic of this reaction: a decrease at 536 nm and the growth of a band at 542 nm. Under such a large excess of NO, the system cleanly forms the reduced ferrous nitrosyl complex (Figure 2), and the spectral changes seen were independent of the buffers used.

Temporal plots of the disappearance of **1** monitored at 422 nm or the appearance of **4** monitored at 412 nm could be fit to exponential functions under these conditions and were in agreement with each other. The k_{obs} values were determined

(19) Forshey, P. A.; Kuwana, T. *Inorg. Chem.* **1981**, *20*, 693−700.
(20) (a) El-Awady, A. A.; Wilkins, P. C.; Wilkins, R. G. *Inorg. Chem.* **1985**, *24*, 2053−2057. (b) Harris, F. L.; Toppen, D. L. *Inorg. Chem.* **1978**, *17*, 71−73.
(21) (a) Laverman, L. E.; Ford, P. C. *J. Am. Chem. Soc.* **2001**, *123*, 11614−11622. (b) Hoshino, M.; Ozawa, K.; Seki, H.; Ford, P. C. *J. Am. Chem. Soc.* **1993**, *115*, 9568−9575. (c) Nakagawa, S.; Yashiro, T.; Munakata, H.; Imai, H.; Uemori, Y. *Inorg. Chim. Acta* **2003**, *349*, 17−22.
(22) Lorkovic, I. M.; Miranda, K. M.; Lee, B.; Bernhard, S.; Schoonover, J. R.; Ford, P. C. *J. Am. Chem. Soc.* **1998**, *120*, 11674−11683.
(23) Laverman, L. E.; Wanat, A.; Oszajca, J.; Stochel, G.; Ford, P. C.; van Eldik, R. *J. Am. Chem. Soc.* **2001**, *123*, 285−293.

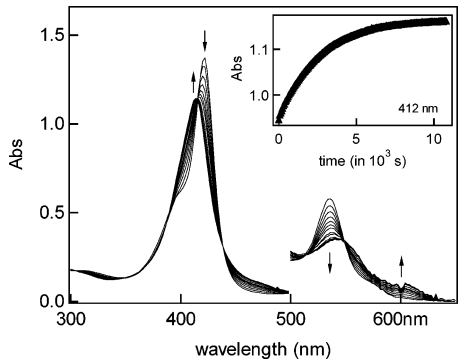

Figure 2. Temporal spectral changes after the introduction of NO (1.9 mM) to Fe^{III}(TPPS) (1.2×10^{-5} M) in pH 4.98 NaOAc/HOAc buffered (80 mM) aqueous solution at 298 K with $\mu_{tot} = 0.10$ M. The first seven spectra were taken at 600 s intervals; subsequent scans were recorded every 1200 s. (Inset) Temporal absorbance trace taken at 412 nm, representing the appearance of Fe^{II}(TPPS)(NO). The data and the fit ($k_{obs} = 3.32 \times 10^{-4}$ s^{-1}) are indistinguishable.

in this manner for the NO reduction under a variety of conditions including a range of [NO] (0−1.9 mM) and several buffers at different pH values. These proved to be modestly sensitive to ionic strength, so most kinetics experiments were carried out at a low μ, generally 0.1 M but sometimes 0.2 M. In all experiments, spectral characteristics were similar to those observed with the phosphate buffer. Within the NaOAc/HOAc buffer system, k_{obs} demonstrated little or no dependence on the pH. For example, the k_{obs} for the reaction of **1** with 1.9 mM NO ($P_{NO} = 1.0$ atm) in pH 5.0 aqueous solution buffered with 20 mM NaOAc/HOAc ($\mu = 0.1$ M) was determined to be $(2.14 \pm 0.37) \times 10^{-4}$ s^{-1}. At pH 4.0, with the same NaOAc/HOAc concentration and ionic strength, $k_{obs} = (2.36 \pm 0.30) \times 10^{-4}$ s^{-1}. Thus, at these relatively low solution pH values, there appears to be no specific base catalysis (by OH^-) of the reductive nitrosylation of Fe^{III}(TPPS). However, the rates were somewhat faster when the reaction was carried out at pH 6.0. For example, k_{obs} was measured to be $(6.8 \pm 0.5) \times 10^{-4}$ s^{-1} in 50 mM phosphate buffer, about 3-fold higher than that measured at pH 5.0. Although a small fraction of this increase can be attributed to the higher buffer concentration (see below), this result suggests that OH^- may contribute to the overall reductive nitrosylation kinetics at this somewhat higher pH as was seen with the ferriheme proteins.[6]

Consistent with the observations of Hoshino et al., the k_{obs} values determined for the reduction to Fe^{II}(TPPS)(NO) under specific conditions increase nearly linearly with NO at low concentrations but approach a limiting value at high [NO]. According to the model described in eqs 4 and 5, the kinetics should follow the behavior indicated by eq 9

$$\frac{d[Fe^{III}]}{dt} = \frac{k_{red}K_{NO}[NO][Fe^{III}]}{1 + K_{NO}[NO]} = k_{obs}[Fe^{III}] \qquad (9)$$

where k_{red} is the rate constant for the reduction of **3** and may represent the sum of several terms dependent on the medium and [Fe^{III}] is the sum of [**1**] and [**3**]. In general, the k_{red} for the nitrosyl complex Fe^{III}(P)(NO) (eq 10) can be calculated from the relationship $k_{red} = \{(1+K_{NO}[NO])/K_{NO}[NO]\}k_{obs}$. For example, a majority of the Fe^{III}(TPPS) experiments were carried out with [NO] = 1.9 mM at 298 K where k_{red} would be 1.4 k_{obs}.

$$Fe^{III}(P)(NO) + H_2O + NO \xrightarrow{k_{red}} Fe^{II}(P)(NO) + NO_2^- + 2H^+ \quad (10)$$

In the pH range of 4−6, k_{red} did prove to be dependent on the identity and concentration of the buffer used. For the linear plot of k_{obs} versus the concentration of the NaOAc/HOAc buffer at 0.1 M ionic strength and $P_{NO} = 1$ atm, a slope of 1.73×10^{-3} M^{-1} s^{-1} and an intercept of 1.95×10^{-4} s^{-1} were found (Supporting Information, Figure S3). This implies the relationship $k_{red} = k_0 + k_{buffer}$[buffer], where k_0 is a buffer-independent term as indicated by the nonzero y intercept. For NaOAc/HOAc at pH 5.0, the buffer-dependent term, $k_{acetate}$ was determined to be $(2.4 \pm 0.1) \times 10^{-3}$ M^{-1} s^{-1} (calculated by multiplying the slope by 1.4 as discussed above), and k_0 was determined to be 2.8×10^{-4} s^{-1}. At the same pH, the buffer DESPEN exhibited similar behavior but with a 5-fold greater slope ($k_{DESPEN} = (1.1 \pm 0.1) \times 10^{-2}$ M^{-1} s^{-1}). Such behavior was previously seen with the NO reduction of the copper(II) complex $Cu(dmp)_2^{2+}$ (dmp = 2,9-dimethyl-1,10-phenanthroline) and was attributed to general base catalysis.[7c] In this context, one may propose a mechanism for the NO reduction of **1** under conditions of general base catalysis as illustrated by Scheme 2.

Similar behavior was seen for phosphate buffer solutions at pH 6.0 (Supporting Information, Figure S4) where a slope of 3.0×10^{-3} M^{-1} s^{-1} ($k_{phosphate} = 4.2 \times 10^{-3}$ M^{-1} s^{-1}) was obtained; however, constant ionic strength was not maintained. In this case, the extrapolated value of k_{obs} at [buffer] = 0 ($k_0 \approx 6 \times 10^{-4}$ s^{-1}) is several times larger than the k_0 found in the pH 5.0 acetate solutions, suggesting that specific base catalysis by OH^- may be contributing at the higher pH. Modest specific base catalysis was demonstrated for the ferriheme protein reductive nitrosylations in pH 7−8 solutions.[6]

Reduction of Fe^{III}(TMPy). The NO reduction of Fe^{III}(TMPy) (**2**) also occurs readily.[8b] Under conditions analogous to those used for the reactions of **1**, the k_{obs} values for the reduction of Fe^{III}(TMPy)/Fe^{III}(TMPy)(NO) solutions to Fe^{II}(TMPy)(NO) proved to be much faster at all pH values examined. For example, the value of k_{obs} recorded for the reductive nitrosylation of **2** in pH 4.5 acetate buffer solution (20 mM) under 1.0 atm of NO was 7×10^{-3} s^{-1}. This is more than an order of magnitude larger than that determined for **1** under analogous conditions.

Catalysis by Nitrite Ion. Our initial kinetics studies suffered reproducibility problems despite considerable efforts to ensure the consistency of the reaction conditions. These problems, however, led us to suspect a possible kinetic role for nitrite, which is not only a reaction product (eq 6) but also a common impurity in aqueous NO solutions.[24] Prepar-

(24) (a) Wolak, M.; Stochel, G.; Hamza, M.; van Eldik, R. *Inorg. Chem.* **2000**, *39*, 2018−2019. (b) Nemes, A.; Pestovsky, O.; Bakac, A. *J. Am. Chem. Soc.* **2002**, *124*, 421−427.

Scheme 2. Proposed Scheme for General Base Catalysis

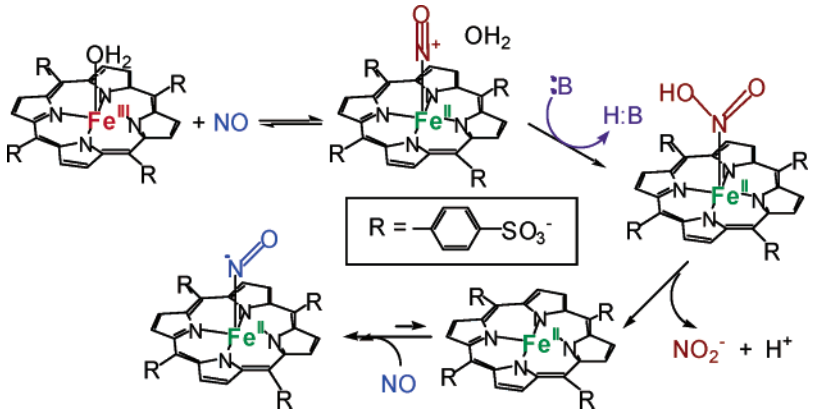

ingsolutions with NO_2^- levels below 50 μM proved difficult to achieve even with strict precautions. The likely source of such contamination is from NO autoxidation[25] by trace amounts of air. The problem is markedly accentuated by the tendency of NO_x impurities to concentrate in the solution phase. The reexamination of the spectra from the early kinetics studies suggested that NO_2^- (at λ_{max} = 354 nm, ϵ = 22.6 M^{-1} cm^{-1}) levels in the aqueous NO solutions were in the range of 40−180 μM (with most samples falling in the range of <100 μM). Although such low levels are rarely attained with aqueous NO solutions, the problems with reproducibility led us to add $NaNO_2$ deliberately to the reaction solution to evaluate its possible catalytic effects on NO reductions of ferrihemes. As will be seen below, the effects of nitrite on the kinetics are profound.

When $NaNO_2$ (0−2.5 mM) was deliberately added to buffered solutions of **1** and NO (NaOAc/HOAc buffer at pH 4.96 with μ_{tot} = 0.1 M and [NO] = 1.9 mM), the rates of Fe^{III} reduction to **4** were dramatically enhanced. The k_{obs} values proved to be a linear function of $[NO_2^-]$ (Supporting Information, Figure S5); that is, $k_{obs} = (k_{red} + k_{nitrite}[NO_2^-])f(NO)$, where $f(NO) = (K_{NO}[NO]/(1 + K_{NO}[NO])$ and is the function described in eq 9 to account for the role of NO under a specified set of conditions. The slope of this plot is 2.2 ± 0.1 M^{-1} s^{-1}. Once the equilibrium formation of Fe^{III}(TPPS)(NO) is taken into account (i.e., f(NO)), the value of the catalytic rate constant $k_{nitrite}$ can be calculated from this slope as 3.1 M^{-1} s^{-1}, more than 3 orders of magnitude larger than the effect of the acetate buffer alone. ($k_{acetate}$ = 2.4 × 10^{-3} M^{-1} s^{-1}.)

In contrast, when millimolar amounts of nitrite (0−100 mM) were added to Fe^{III}(TPPS) in the absence of added NO, no reduction of **1** to **4** could be seen spectroscopically. Thus, nitrite is indeed a catalyst for the NO reduction of Fe^{III}(TPPS). Because NO_2^- is also a reaction product, the system is, in principle, autocatalytic, although the very small concentrations of ferric porphyrin present would lead to very low concentrations of NO_2^- formed via the reaction stoichiometry.

The functional dependence of the nitrite-catalyzed reductive nitrosylation rates on NO concentration that is consistent with eq 8 was demonstrated for Fe^{III}(TPPS) in pH 5.0 aqueous NaOAc/HOAc buffer (20 mM) solution by measuring the k_{obs} values for the NO reduction of **1** at a fixed NO_2^- concentration (2.0 mM) but varing [NO]. The rates increased with [NO] but approached a limiting value. According to eq 9, a double-reciprocal plot (k_{obs}^{-1} vs $[NO]^{-1}$) should be linear with a nonzero intercept equal to k_{red}^{-1} and a slope equal to $(K_{NO}k_{red})^{-1}$. This plot is shown in Figure 3, from which the values k_{red} = (7.2 ± 0.4) × 10^{-3} s^{-1} and K_{NO} = 1.39 × 10^3 M^{-1} were obtained. The latter is within the experimental uncertainty of the K_{NO} values measured for Fe^{III}(TPPS) from the spectral changes under varied P_{NO} at pH 5 (see above) and by other workers.[21] The k_{red} term equals k_0 + k_{buffer}[buffer] + $k_{nitrite}[NO_2^-]$; however, under these conditions, $k_{nitrite}[NO_2^-]$ is more than an order of magnitude larger than the sum of the other two.

The catalytic rate constant $k_{nitrite}$ proved to be independent of the buffer solution in which the experiment was conducted. A plot similar to that shown in Figure S5 of the Supporting

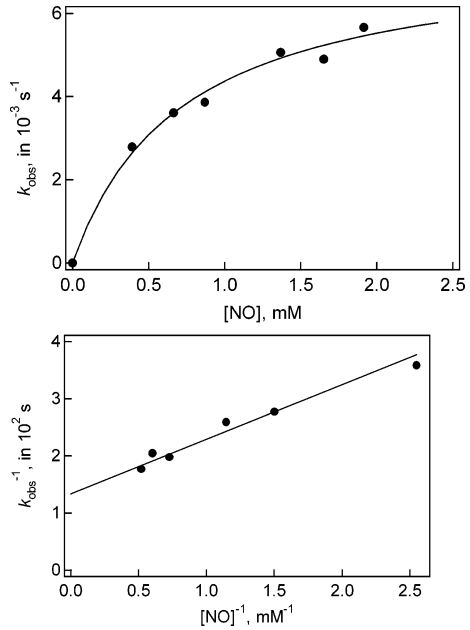

Figure 3. (Upper) Plot of k_{obs} versus [NO] from the NO reduction of Fe^{III}(TPPS) with varying [NO] (0−1.92 mM) using 50 mM NaOAc/HOAc, μ_{tot} = 0.35 M, pH 4.99 at 298 K with added $NaNO_2$ (2.01 mM). (Lower) Plot of k_{obs}^{-1} versus $[NO]^{-1}$ (same data). From this linear plot, a K_{NO} value of (1.39 ± 0.27) × 10^3 M^{-1} was determined.

(25) Ford, P. C.; Wink, D. A.; Stanbury, D. M. *FEBS Lett.* **1993**, *326*, 1−3.

Information was determined for the nitrite catalysis in the DESPEN buffer at pH 5.0 with $\mu = 0.1$ M at 298 K. The slope in this medium was determined to be 2.4 ± 0.1 M^{-1} s^{-1}. Taking into account the equilibrium constant for NO association and the proposed model, we obtained an adjusted nitrite-catalysis rate constant of $k_{nitrite} = 3.4$ M^{-1} s^{-1} in the DESPEN buffer solution, which was experimentally equivalent to that measured in acetate buffer at the same pH.

Nitrite catalysis was also seen for the NO reduction of Fe^{III}(TMPy). This system is sufficiently more reactive, requiring stopped-flow kinetics techniques to measure relevant k_{obs} values over a range of [NO_2^-]. By using the stopped-flow spectrophotometer, solutions of Fe^{III}(TMPy) (8.5×10^{-5} M) in pH 5.0 NaOAc/HOAc buffer solution ($\mu_{tot} = 0.10$ M) were mixed with similarly buffered NO solutions (2.0 mM) containing $NaNO_2$ at various concentrations (10−50 mM) at 298 K. Again, linear plots of k_{obs} versus [NO_2^-] with near-zero intercepts were obtained (Supporting Information, Figure S6). The slopes of these plots reproducibly fell in the range of 24.6 ± 0.9 M^{-1} s^{-1}, and from these slopes and the relationship between k_{obs} and k_{red} described above, the $k_{nitrite}$ value of 83 ± 5 M^{-1} s^{-1} was obtained for the NO reduction of Fe^{III}(TMPy). Notably, this value is nearly 30-fold larger than that obtained for Fe^{III}(TPPS).

Nitrite Catalysis of Ferriheme Protein Reduction. The observation of nitrite catalysis with Fe^{III}(TPPS) and Fe^{III}(TMPy) led us to reexamine the NO reductions of ferriheme proteins metHb and metMb. These kinetics experiments were carried out in pH 7.0 aqueous phosphate buffer solutions at 298 K at constant ionic strength ($\mu = 0.20$ M) with various $NaNO_2$ concentrations under an atmosphere of NO (1.8 mM). Protein concentrations were 7×10^{-6} M (metHb) and 2.7×10^{-5} M (metMb). Consistent with the earlier studies by Hoshino et al.,[6] reactions carried out in pH 7.0 solution in the absence of added nitrite (and in a manner to minimize adventitious NO_2^-) showed that metHb and metMb underwent slow reductive nitrosylation but that the reaction was considerably slower for the latter. Upon mixing, the protein solutions react rapidly with NO to generate an equilibrium mixture of the ferriheme protein and its nitrosyl complex. Under these conditions, this fast process was followed by the slow formation of the ferrous analogues Hb(NO) and Mb(NO), with lifetimes of 10^3 and 10^4 s, respectively. However, in the presence of added $NaNO_2$ (0−20 mM for metHb; 0−80 mM for metMb), the rates dramatically increased, consistent with the catalytic role of NO_2^- in these systems as well. Figure 4 displays typical spectral changes, and Figure S7 in the Supporting Information illustrates the linear dependence of the k_{obs} values for the NO reductions of metHb and metMb proteins under these conditions.

The slopes of these plots are 0.13 ± 0.01 and $(1.09 \pm 0.10) \times 10^{-2}$ M^{-1} s^{-1} for metHb and metMb, respectively. Taking into account the equilibrium constants for the formation of the nitrosyl ferriheme protein complexes metHb(NO) ($K_{NO} = 1.3 \times 10^4$ M^{-1})[6] and metMb(NO) (1.4×10^4 M^{-1}),[21b,23] the catalytic rate constants $k_{nitrite}$ would be calculated as 0.14 ± 0.01 M^{-1} s^{-1} for metHb and $(1.1 \pm 0.1) \times 10^{-2}$ M^{-1} s^{-1} for metMb according to eq 9. Similar to the heme models described above, in the absence of NO, there was no reduction of metHb or metMb by the added nitrite alone. However, the possible formation of nitrite complexation to the ferric centers needs to be considered. (See below.)

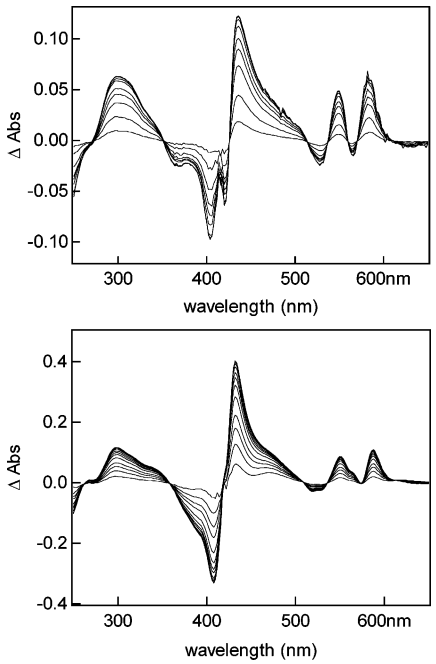

Figure 4. (Upper) Difference spectra recorded upon the reaction of NO (1.8 mM) with metHb (7×10^{-6} M) in pH 6.99 phosphate buffer solution (41.3 mM) with [$NaNO_2$] = 20 mM, $\mu_{tot} = 0.20$ M, 298 K. (Lower) Difference spectra for the reaction of NO (1.8 mM) with metMb (2.71×10^{-5} M) in pH 7.00 phosphate buffer solution (50.3 mM) with [$NaNO_2$] = 20 mM, $\mu_{tot} = 0.20$ M, $T = 298$ K. For both metHb and metMb, the first spectrum is taken after 60 s. The next trace is taken after 150 s. The three subsequent spectra are taken at 150-s intervals. The sixth and seventh spectra are taken after 900 and 1500 s, respectively. The remaining spectra were recorded at 600 s intervals.

Nitrite Binding to Fe^{III}(Por) Models. NO_2^- has recently been shown to bind to metHb and metMb with equilibrium constants of 223 and 42.4 M^{-1}, respectively, at 298 K.[26] With this in mind, we instituted studies to evaluate the possible nitrite ion binding to heme model systems Fe^{III}(TPPS) and Fe^{III}(TMPy) (eq 10). These studies were carried out at pH 5 to reduce possible complications arising from hydrolysis or dimerization of the Fe^{III}(P) aquo complexes at higher pH values and nitrite protonation at lower pH values (pK_a (HNO_2) 3.37).[27] The concentrations of the ferriheme complexes were 1×10^{-4} M in each case, and spectral changes in these solutions as a function of added NO_2^- were evaluated over the ranges of 0−800 and 0−600 mM for **1** and **2**, respectively. For both complexes, only very small changes in the UV−vis spectra were seen for [NO_2^-] ≤ 50 mM, a range where the catalysis of NO reduction was clearly evident. However, at higher [NO_2^-], there were progressive spectra changes indicating the formation of complexes, presumably via the displacement of an axial water of

(26) Wanat, A.; Gdula-Argasinska, J.; Rutkowska-Zbik, D.; Witko, M.; Stochel, G.; van Eldik, R. *J. Biol. Inorg. Chem.* **2002**, *7*, 165−176.
(27) Weast, R. C., Ed. *Handbook of Chemistry and Physics*, 67th ed.; CRC Press: Boca Raton, FL, 1986; p D-163.

Scheme 3. Dead-End Equilibrium

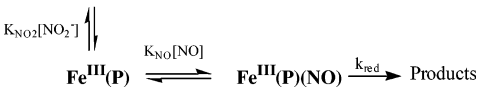

$Fe^{III}(P)(H_2O)_2$. The treatment of these data by standard methods gave small $K_{NO_2^-}$ values of ~3 and <10 M^{-1} at 298 K for **1** and **2**, respectively, values that are much smaller than those reported for the ferriheme proteins.[26] (The approximate values of $K_{NO_2^-}$ described above are the result of the high nitrite concentrations necessary to effect complex formation.)

$$Fe^{III}(P) + NO_2^- \overset{K_{NO_2^-}}{\rightleftharpoons} Fe^{III}(P)(NO_2^-) \qquad (11)$$

One model for the potential kinetics effect of eq 11 would be to treat this as a nitrite "dead-end" equilibrium that inhibits reaction with NO as illustrated in Scheme 3. In that model, the formation of ferric nitrosyl complexes is inhibited by the competition with nitrite for the coordination site. However, whereas such competition might be expected for metHb and metMb, which have a proximal histidine ligand so there is only one potential NO coordination site, it is not clear what the effect might be for **1** and **2** because these each have two axial sites available for NO coordination. In the case of Scheme 3, the rate law would still have the form $k_{obs} = (k_{red} + k_{nitrite}[NO_2^-])\, f(NO)$, but in this case, $f(NO) = (K_{NO}[NO]/(1 + K_{NO}[NO] + K_{NO_2^-}[NO_2^-])$. The significance of such inhibition (if any) would therefore be based on the relative magnitudes of $K_{NO_2^-}[NO_2^-]$ versus the rest of the denominator, $1 + K_{NO}[NO]$. Given the large values of K_{NO} for the ferriheme systems described here, any such inhibition must be small in each case because the rate studies that probed the catalytic role of nitrite were carried out at relatively high [NO] (1.9 mM). For example, among the systems studied metMb (42.4 M^{-1}) and metHb (223 M^{-1}) display the largest values of $K_{NO_2^-}$, and the catalytic role of nitrite was examined over the respective concentration ranges of 0−80 and 0−20 mM. At the highest $[NO_2^-]$ for which nitrite catalysis was probed for these two systems, the respective values of $K_{NO_2^-}[NO_2^-]$ were 3.4 and 4.5; by comparison, values of $1 + K_{NO}[NO]$ would be 24.4 and 26.2 under the conditions studied. Thus, we conclude that the formation of nitrite complexes according to a dead-end equilibrium of the type indicated by Scheme 3 would have, at most, a minor effect on the overall rates of the ferriheme reductions by NO described here.

Possible Mechanisms of Nitrite Catalysis. There are two limiting mechanisms by which we can envision nitrite catalysis to occur. The first (Scheme 4) would be inner sphere in nature where NO_2^- serves as the primary nucleophile toward the Fe^{III}-coordinated nitrosyl to give an intermediate $Fe^{II}-N_2O_3$ complex. The dissociation of the intermediate releases the ferroheme complex or protein plus N_2O_3, which should undergo hydrolysis in aqueous solution to nitrous acid.[28] The ferroheme intermediate is then trapped by excess NO to produce the $Fe^{II}(P)(NO)$ final product. This mechanism follows the general theme discussed above with regard to specific and general base catalysis; however, there is no obvious reason why aqueous NO_2^- should have the unusual nucleophilicity necessary for such a catalytic pathway.

Scheme 4. Inner-Sphere Mechanism for Nitrite Catalysis

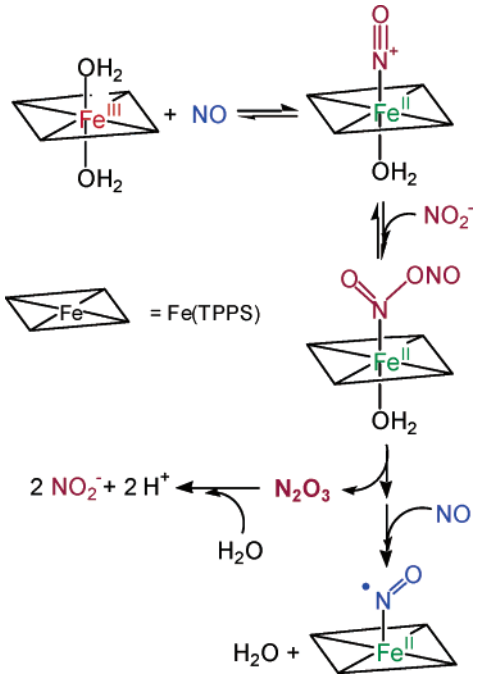

Scheme 5. Outer-Sphere Electron-Transfer Mechanism for Nitrite Catalysis

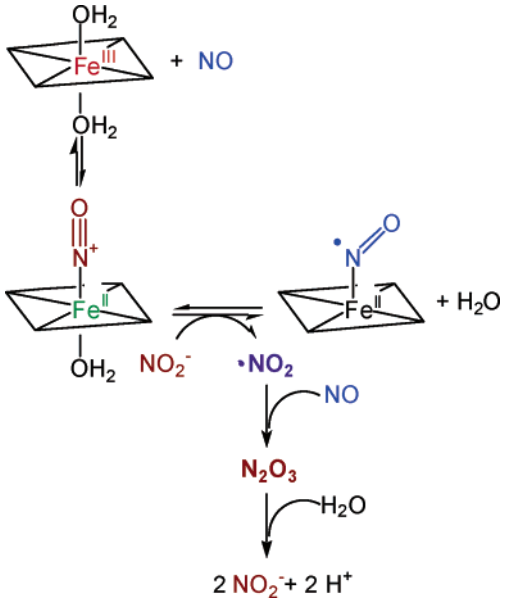

A markedly different mechanism is proposed in Scheme 5. The key step in this scheme would be the direct reduction of the ferriheme nitrosyl to the ferroheme analogue by outer-sphere electron transfer from NO_2^-. The other product would be nitrogen dioxide, $NO_2^{\bullet}$, and this would be rapidly scavenged by the reaction with excess NO ($k = 1.1 \times 10^9$ M^{-1} s^{-1})[29] to give N_2O_3, an intermediate with the same

(28) (a) Graetzel, M.; Henglein, A.; Lilie, J.; Beck, G. *Ber. Bunsen-Ges. Phys. Chem.* **1969**, *73*, 646−653. (b) Graetzel, M.; Taniguchi S.; Henglein, A. *Ber. Bunsen-Ges. Phys. Chem.* **1970**, *74*, 488−493.

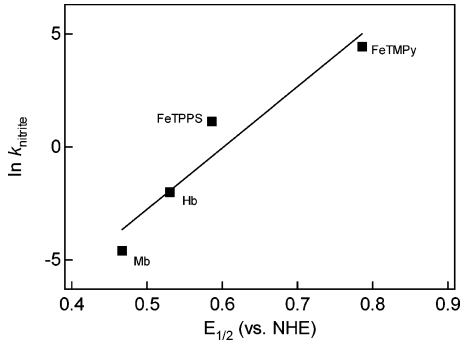

Figure 5. Plot of ln($k_{nitrite}$) vs $E_{1/2}$ (V), where $k_{nitrite}$ is the catalytic rate constant for the nitrite catalysis of reductive nitrosylation and $E_{1/2}$ represents the known or estimated (see text) reduction potentials for the nitrosyl ferriheme complexes: Fe^{III}(TPPS)(NO), Fe^{III}(TMPy)(NO), metHb(NO), and metMb(NO).

composition as that proposed for the inner-sphere mechanism. Again, the latter would be subject to hydrolysis to give the nitrite product. The key step here is the electron transfer, and although this is not thermodynamically favored ($\Delta E = -0.31$ V), the fast trapping of one of the initial products, $NO_2^{\bullet}$, and subsequent N_2O_3 hydrolysis may make it viable.

The potential role of an outer-sphere electron transfer as the rate-limiting step may be evaluated by using the Marcus cross relation[30] to estimate the rate constant for the second-order reaction between Fe^{III}(P)(NO) and NO_2^-. From the Marcus cross relation, $k_{OS} \approx (k_{11}k_{22}K_{OS})^{1/2}$, where k_{11} is the rate constant for Fe^{II}(P)(NO)/Fe^{III}(P)(NO) self-exchange, k_{22} is that for NO_2^-/NO_2 self-exchange via outer-sphere electron transfer (0.3 M^{-1} s^{-1}),[31] and K_{OS} is the equilibrium constant of the electron-transfer step (6×10^{-6} for P = TPPS).[32] Accordingly, for $k_{OS} = k_{nitrite}$, the calculated value for k_{11} for P = TPPS would need to be $\sim 6 \times 10^6$ M^{-1} s^{-1}. This estimated value falls within the range of the previously observed self-exchange rates of low-spin Fe porphyrin complexes;[33] however, it is important to recognize that the $Fe^{III/II}$(TPPS)(NO) self-exchange rate constant is unknown. Furthermore, unlike other low-spin ferriheme/ferroheme couples, the nitrosyl complexes may be subject to reorganization energy contributions resulting from the different configurations (linear and bent, respectively) of the Fe−NO bond in the two oxidation states.[12]

If an outer-sphere-type mechanism is viable for the nitrite catalysis of Fe^{III}(P) reduction, then the rate constant $k_{nitrite}$ should be a function of the Fe^{III}(P)(NO)/Fe^{II}(P)(NO) reduction potentials $\Delta E_{1/2}(Fe^{III}/Fe^{II})$. This is derived from the Marcus cross relation becasue k_{OS} is proportional to $K_{OS}^{1/2}$ if the rather large assumption is made that k_{11} is approximately constant for different hemes. In this context, a plot of ln($k_{nitrite}$) versus $\Delta E_{1/2}(Fe^{III}/Fe^{II})$ should be linear. Figure 5 is such a plot, and the predicted pattern is roughly

Scheme 6. Born−Haber-Type Cycle to Estimate the Reduction Potential for Nitrosyl Complexes of Ferriheme Proteins

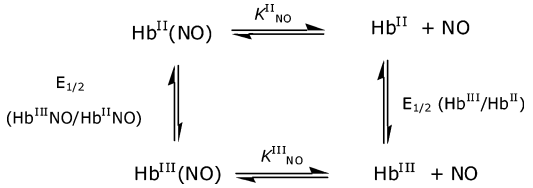

demonstrated. The four points on this plot include the two model compounds for which the $\Delta E_{1/2}(Fe^{III}/Fe^{II})$ are well characterized. To our knowledge, direct measurements of the metHb(NO)/Hb(NO) and metMb(NO)/Mb(NO) half-cell reduction potentials have not been reported, but estimates of 0.49−0.57 and 0.47 V (vs NHE), respectively, were generated from known reduction potentials and equilibrium constants[6,27,34] using Born−Haber-type cycles (Scheme 6). The values estimated correlate with the $k_{nitrite}$ trend: Fe^{III}(TMPy) > Fe^{III}(TPPS) > $metHb^T$ > metMb. Quantitatively, Figure 5 is less convincing because the slope of that plot is 27.8 V^{-1}, whereas the predicted slope would be 38.9 V^{-1}. Nonetheless, such a difference can easily be attributed to the assumptions inherent in our use of the Marcus cross-relation treatment as well as the uncertainties in the ferriheme protein reduction potentials. Thus, the qualitative agreement is consistent with the outer-sphere electron-transfer mechanism (Scheme 5).

Summary and Commentary. Nitrite ion catalysis of reductive nitrosylation has been demonstrated for heme model complexes Fe^{III}(TPPS) and Fe^{III}(TMPy) as well as for ferriheme proteins metHb and metMb. The increased sensitivity of the kinetics to the Fe^{III}(P)(NO) reduction potential is consistent with the behavior expected for an outer-sphere electron-transfer mechanism; however, an inner-sphere process may also be sensitive to the overall driving force of the reaction, as reflected by this parameter. Nitrite is one of the products of NO autoxidation in aqueous solution[24] and is a ubiquitous component of experiments when aqueous NO is added to an aerobic system to study biological effects and should not be assumed to be innocuous. For example, reactions of NO and red blood cells or metHb have been reported to give SNO-Hb.[10,11] It has been argued that this product may be the result of the direct transfer of a NO^+ moiety from the iron center to the β-cysteine-93 thiol. However, according to the crystal structure data,[35] the distance between the two sites is quite large, so a direct reaction of the cysteine-SH with the coordinated NO does not appear to be likely. However, both the inner- and outer-

(29) Treinin, A.; Hayon, E. *J. Am. Chem. Soc*. **1970**, *92*, 5821−5828.
(30) Marcus, R. A. *J. Phys. Chem*. **1968**, *72*, 891−899.
(31) Stanbury, D. M. In *Electron Transfer Reactions*, Isied, S. S., Ed.; Advances in Chemistry Series 253; American Chemical Society: Washington, DC, 1997; pp 165−182.
(32) Pearson, R. G. *J. Am. Chem. Soc.* **1986**, *108*, 6109−6114.
(33) (a) Shirazi, A.; Barbush, M.; Ghosh, S.; Dixon, D. W. *Inorg. Chem*. **1985**, *24*, 2495−2502 (b) Pasternack, R. F.; Spiro, E. G. *J. Am. Chem. Soc*. **1978**, *100*, 968−972.
(34) (a) The equilibrium constant for the formation of Fe^{II}(P)(NO) is 8.7 $\times 10^9$ M^{-1} for $metHb^T$, 1.7 $\times 10^{11}$ M^{-1} for $metHb^R$, and 1.4 $\times 10^{11}$ M^{-1} for metMb.[5e] The reduction potential for metHb is 0.144 V (vs NHE) and for metMb is 0.06 V (vs NHE).[34b] Electrochemical studies in this laboratory agree with the estimated reduction potential for metHb(NO) ($\sim$0.530 V vs NHE).[34c] (b) Fasman, G. D., Ed. *Handbook of Biochemistry and Molecular Biology*; CRC Press: Cleveland, OH, 1976; pp 131−150. (c) Kilnic, M. E.; Fernandez, B. O., unpublished work.
(35) Chan, N.-L.; Rogers, P. H.; Arnone, A. *Biochemistry* **1998**, *37*, 16459−16464. According to the crystallographic data of SNO-Hb (1BUW), the shortest separation between iron and β-cysteine 93 is at least 10 Å. The potential for NO^+ transfer from the heme at this distance would not be high during the structural transition from R to T.

sphere mechanisms described above for nitrite catalysis call for the intermediacy of N_2O_3, a known nitrosating agent. Although N_2O_3 is known to undergo hydrolysis, this reaction has a roughly millisecond lifetime in aqueous solution that is likely to be longer in the hydrophobic pocket of a heme protein. Thus, if the reaction were catalyzed by nitrite, then N_2O_3 formation at the heme site could easily lead to protein modification such as β-cys-93 nitrosation. If one considers the (very low) NO concentrations present under normal physiological conditions in the cardiovascular system, then the generation of SNO-Hb via such pathways may not be relevant under such circumstances. However, in experiments where a bolus of NO is added to Hb or red blood cell solutions, the higher localized concentrations of NO might well lead to products resulting from the intermediacy of N_2O_3.

In summary, the unexpected catalysis pathway described further emphasizes the potentially important roles of NO_x intermediates in biological transformations often attributed to NO alone.

Acknowledgment. This work was supported by the U.S. National Science Foundation (CHE0095144). We thank Chosu Khin, Mark Lim, undergraduate Joy Jackson (URCA Grant), and Kelly McCord (CNSI Apprentice Researcher) for experimental measurements relevant to the results reported. B.O.F. thanks the UCSB Graduate Division for a Graduate Opportunity Fellowship and a Dissertation Fellowship.

Supporting Information Available: Figures showing spectral changes, an equilibrium plot, the effects of buffers on rate constants, and the effects of nitrite catalysis. This material is available free of charge via the Internet at http://pubs.acs.org.

IC049532X